1WP

NASA TECHNICAL MEMORANDUM

NASA TM X- 71926

COPY NO.

NASA TM X-

Plane-Stress Fracture of Compact and Notch-Bend Specimens

by J. C. Newman, Jr.
Langley Research Center
Hampton, Virginia 23665

TECHNICAL PAPER presented at the 10th Anniversary Meeting of the Society of Engineering Science, Raleigh, North Carolina, Nov. 5-7, 1973.

NATIONAL AERONAUTICS AND SPACE ADMINISTRATION
LANGLEY RESEARCH CENTER, HAMPTON, VIRGINIA 23665

19

1. Report No.	2. Government Accession No.	3. Recipient's Catalog No.
NASA TM X-71926		

4. Title and Subtitle	5. Report Date
Plane-Stress Fracture of Compact and Notch-Bend Specimens	February 1974
	6. Performing Organization Code
7. Author(s)	8. Performing Organization Report No.
J. C. Newman, Jr.	
9. Performing Organization Name and Address	10. Work Unit No.
NASA Langley Research Center Hampton, VA 23665	501-22-02-01-00
	11. Contract or Grant No.
12. Sponsoring Agency Name and Address	13. Type of Report and Period Covered
National Aeronautics and Space Administration Washington, D.C. 20546	Technical Memorandum
	14. Sponsoring Agency Code

15. Supplementary Notes

Paper presented at the 10th Anniversary Meeting of the Society of Engineering Science, November 5 - 7, 1973.

16. Abstract

Thin-gaged or high toughness materials containing cracks usually fail in a ductile manner with nominal failure stresses approaching the ultimate strength of the material. For such materials, a two-parameter fracture criterion was developed. An equation which related the linear elastic stress-intensity factor, elastic nominal stress, and two material parameters has previously been derived and has been used as a fracture criterion for surface- and through-cracked specimens under tensile loading. In the present paper the two-parameter fracture criterion was rederived in a more general form and was extended to compact and notch-bend fracture specimens. A close correlation was found between experimental and predicted failure stresses.

17. Key Words (Suggested by Author(s)) (STAR category underlined)	18. Distribution Statement
FRACTURE STRESS-INTENSITY FACTOR STRUCTURAL MECHANICS MATERIALS (METALLIC)	Unclassified - Unlimited

19. Security Classif. (of this report)	20. Security Classif. (of this page)	21. No. of Pages	22. Price*
Unclassified	Unclassified	19	NTIS

*Available from { The National Technical Information Service, Springfield, Virginia 22151
STIF/NASA Scientific and Technical Information Facility, P.O. Box 33, College Park, MD 20740

ABSTRACT

Thin-gaged or high toughness materials containing cracks usually fail in a ductile manner with nominal failure stresses approaching the ultimate strength of the material. For such materials, a two-parameter fracture criterion was developed. An equation which related the linear elastic stress intensity factor, elastic nominal stress, and two material parameters has previously been derived and has been used as a fracture criterion for surface and through-cracked specimens under tensile loading. In the present paper the two-parameter fracture criterion was rederived in a more general form and was extended to compact and notch-bend fracture specimens. A close correlation was found between experimental and predicted failure stresses.

PLANE-STRESS FRACTURE OF COMPACT AND NOTCH-BEND SPECIMENS

J. C. Newman, Jr.
NASA-Langley Research Center, Hampton, VA 23665

INTRODUCTION

In many applications, thin-gaged or high toughness materials are necessary for efficient and light-weight structures. These materials, in the presence of cracks, usually fail in a ductile mode involving large inelastic crack-tip deformations. As a result, the widely-used concepts of Linear Elastic Fracture Mechanics (LEFM) often do not apply. To obtain fracture criteria for these materials, the elastic-plastic behavior at the crack tip must be considered.

Several equations have been proposed for calculating the elastic-plastic stress-strain behavior at notches and cracks. For notches, equations have been derived by Hardrath and Ohman [1] and by Neuber [2]. For cracks, equations have been derived by Hutchinson [3] and by Rice and Rosengren [4]. The Hardrath-Ohman relation was generalized for a cracked plate by Kuhn and Figge [5]. In a similar way, Newman [6] used Neuber's relation to derive an equation which related the linear elastic stress-intensity factor, elastic nominal stress, and two material parameters. This equation was used as a Two-Parameter Fracture Criterion (TPFC) in [6] to analyze failure of surface- and through-cracked sheet and plate specimens under tensile loading.

In the present paper the TPFC has been rederived in a more general form and has been extended to compact and notch-bend specimens. The

application of the TPFC to such specimens was evaluated by using fracture data on two steels and two aluminum alloys.

SYMBOLS

a	initial crack length, mm
E	Young's modulus, MN/m^2
$F(a/W)$	stress-intensity correction factor based on nominal stress
K_F	fracture toughness computed from eq. (4), $MN/m^{3/2}$
K_{Ie}	elastic stress-intensity factor at failure, $MN/m^{3/2}$
L	major span length for notch-bend specimen, mm
m	fracture toughness parameter
P	applied load, N
r^*	characteristic length parameter for a crack, mm
S_n	elastic nominal (net-section) stress, MN/m^2
S_u	maximum value of elastic nominal stress, MN/m^2
t	specimen thickness, mm
W	specimen width, mm
ε_f	local fracture strain
σ_f	local fracture strength, MN/m^2
σ_u	ultimate tensile strength, MN/m^2
σ_{ys}	yield stress (0.2 percent offset), MN/m^2

TWO-PARAMETER FRACTURE CRITERION

The elastic stress distribution in front of a crack tip ($\theta = 0$) in a finite plate subjected to symmetric inplane loading has the general form

$$\sigma_{\theta\theta} = C_1 \frac{K_I}{\sqrt{r}} + C_2 + C_3 \left(\frac{r}{a}\right)^{\frac{1}{2}} + \cdots \qquad (1)$$

where the coordinate system (r,θ) is shown in Fig. (1). The coefficient C_1 is a constant and the other C's depend upon the applied loading and configuration. Near the crack tip the first term dominates because of the singular behavior in stresses. The determination of the stress-intensity factor, K_I, is the basis for LEFM. The stress-intensity factor is a function of loading, configuration, size and location of the crack. In this study, the stress-intensity factor was expressed as

$$K_I = S_n \sqrt{\pi a}\ F(a/W) \qquad (2)$$

The application of LEFM to fracture has a number of limitations. One is that as the crack size approaches zero, the stresses in front of the crack tip, expressed only as the first term in eq. (1), also approach zero instead of the nominal stress. Therefore, additional terms in eq. (1) must be included in the analysis. Secondly, the use of LEFM is restricted to conditions in which the plastic deformations at the crack tip are very small (plane-strain fracture [7]). For such cases, K_{Ie}, the critical elastic stress intensity factor, is found to be constant (K_{Ic}). However, when large plastic deformations occur at the crack tip K_{Ie} varies with planar dimensions, such as crack length or specimen width [8]-[10]. To

extend the analysis to cases involving large plastic deformations the elastic-plastic behavior near the crack tip must be considered.

Neuber [2] analyzed the elastic-plastic stresses and strains in shear-strained bodies with notches and concluded that the product of stress- and strain-concentration was equal to the elastic stress concentration squared. Experimentally, Crews [11] has shown that Neuber's equation represents the local stress-strain behavior of notched sheet specimens. Theoretically Rice and Rosengren [4] and Hutchinson [3] have shown that Neuber's equation also applies for the local crack-tip elastic-plastic stress-strain behavior.

In this study, Neuber's equation was written as $\sigma \epsilon E = \sigma_e^2$ where σ and ϵ are the local stress and strain, respectively, and σ_e is the local elastic stress. The local elastic stresses were obtained from eq. (1). Substituting eq. (1) into Neuber's equation and neglecting terms of order $\left(\frac{r}{a}\right)^{1/2}$ gave

$$\frac{1}{C_1}\sqrt{r\,\sigma\,\epsilon\,E} = \frac{K_I}{1 - \frac{C_2}{\sqrt{\sigma\epsilon E}}} = \frac{K_I}{1 - \frac{\sigma_u}{\sqrt{\sigma\epsilon E}}\left(\frac{S_n}{\beta\sigma_u}\right)} \qquad (3)$$

The coefficient C_2 is a linear function of the elastic nominal stress and, therefore, was rewritten as a constant $(1/\beta)$ times this stress. The ultimate strength was introduced to nondimensionalize the nominal stress.

When eq. (3) is applied to fracture, the local σ and ϵ are assumed to reach their critical values σ_f and ϵ_f over a volume of material which is

characterized by r* (see [12]). Redefining those terms in eq. (3) which contain constants, as was done in [6], and writing $\beta\sigma_u$ as S_u gives

$$K_F = \frac{K_{Ie}}{1 - m\left(\frac{S_n}{S_u}\right)} \qquad \text{for } S_n < S_u \tag{4}$$

where K_F and m are the two material parameters. The value of S_u was chosen as the maximum possible elastic nominal stress and was computed from the load required to produce the ultimate stress on the complete net section.

In eq. (4), if m equals zero, K_F equals the elastic stress-intensity factor and the equation is applicable to low-toughness materials (plane-strain fracture). If m equals unity, the equation is similar to that obtained by Kuhn [9] and is applicable to high-toughness materials. Thus, the fracture toughness parameter, m, describes the crack sensitivity of the material.

In the application of eq. (4) to compact and notch-bend specimens, see fig. (2), the stress-intensity factor, nominal stress and S_u must be determined. For the notch-bend specimens, the stress intensity was given by eq. (2) where

$$S_n = 3PL/[2t\ (W - a)^2] \tag{5}$$

and

$$F(a/W) = (1 - \tfrac{a}{W})^2\ \ f(a/W)\ /\sqrt{\pi} \tag{6}$$

The function f(a/W) was given in [7]. The maximum value of elastic nominal stress, S_u, was computed from the load required to produce a fully plastic hinge on the net section and was $1.5\ \sigma_u$.

For the compact specimen, the stress intensity was also given by eq. (2) where

$$S_n = \frac{P}{t(W - a)} \left[1 + 3 \frac{W + a}{W - a}\right] \qquad (7)$$

and

$$F(a/W) = \sqrt{\frac{W}{\pi a}} \left(1 - \frac{a}{W}\right) f(a/W) \; / \; \left[1 + 3 \frac{W + a}{W - a}\right] \qquad (8)$$

The function f(a/W) was given in [13] and [14]. The maximum nominal stress, S_u, was again computed from the load required to produce a fully plastic hinge on the net section under combined tension and bending loads and was given by

$$S_u = \left\{ \left[\sqrt{1 + \left(\frac{W + a}{W - a}\right)^2} - \left(\frac{W + a}{W - a}\right)\right] \left[1 + 3 \left(\frac{W + a}{W - a}\right)\right] \right\} \sigma_u \qquad (9)$$

For a range of a/W between 0.2 and 0.8, $S_u = 1.61 \sigma_u$, agrees to within 4 percent of that given by eq. (9).

After the material parameters K_F and m have been determined from fracture tests, eq. (4) can be used to predict failure stresses for other configurations. The nominal failure stress as a function of crack length, specimen width, and the material parameters was calculated from eq. (2) and (4) as

$$S_n = K_F / \left[\sqrt{\pi a} \; F(a/W) + \frac{m K_F}{S_u} \right] \qquad (10)$$

Eq. (10) was applied for nominal stresses up to the maximum nominal stress, S_u. For small cracks or large a/W ratios, eq. (10) predicts that the nominal

failure stress equals or exceeds S_u. In those cases, the nominal failure stress was set equal to S_u.

ANALYSIS OF TEST DATA

Fracture data for aluminum alloy compact specimens and steel notch-bend specimens were analyzed using eq. (4). The fracture parameters, K_F and m, were determined from the fracture data using a best-fit procedure [6]. This section presents fracture data in terms of the critical elastic stress-intensity factor, K_{Ie}, for a range of crack lengths and specimen widths.

Compact Specimens

Kaufman and Nelson [10] conducted fracture tests on 2219-T851 aluminum alloy compact specimens for various thicknesses, widths, and crack lengths. Fig. (3) shows the results for 13mm-thick specimens with a/W = 0.5 (symbols). The critical stress-intensity factors were computed from the maximum load at failure and the initial crack length. The solid curves show the calculated results based on eq. (4) for several values of a/W. The K_{Ie} values are asymptotically approaching the fracture toughness K_F (indicated by dash-dot line) as the specimen width increases.

The results for 38mm-thick specimens with various a/W ratios and a constant width (W = 150mm) are shown in fig. (4) as symbols. The fracture parameters K_F and m were obtained from fracture data in which the a/W ratio was held constant at 0.5 and the specimen width was varied from 75 to 150mm. Since the fracture parameters were obtained from tests on specimens with constant a/W, they cannot automatically account for the influence of a/W on K_{Ie}. Therefore, the fracture analysis must account for the influence. The solid curve in fig. (4) shows the predictions based on eq. (4). The

agreement between predicted and experimental results for a/W ratios less than 0.5 is considered good and illustrates the ability of the TPFC to account for the influence of a/W on fracture. For a/W ratios greater than 0.8, the critical K_{Ie} values are predicted to decrease rapidly as a/W increases. The dashed curve shows where S_n became equal to S_u.

Notch-Bend Specimens

Jones and Brown [13] conducted fracture tests on three-point notch-bend specimens of 4340 steel at several strength levels. These tests were conducted to determine the effects of thickness, crack length, and specimen width on fracture toughness. Fig. (5) shows the results for 1.5mm-thick specimens for various widths with a/W = 0.5 and L/W ratios of either 4 or 8 (symbols). Although this material had a high ultimate strength, it exhibited an extremely ductile failure (m = 1) because of the thin-gaged tested. The solid curves were calculated from the TPFC for a/W = 0.5 and L/W equal either 4 or 8.

Fig. (6) shows the results for a lower strength 4340 steel than that shown in fig. (5). The results are presented as K_{Ie} plotted against a/W ratio for a constant width specimen (W = 50mm). The solid curve is the predicted behavior based on eq. (4). Again, the dashed curves represent fracture for which S_n equals S_u. A close correlation between experimental and calculated results illustrates how the TPFC can account for the influence of crack length on fracture.

CONCLUDING REMARKS

The Neuber stress-concentration equation was generalized for a crack in a finite plate. An equation was derived which related the linear elastic stress-intensity factor, the elastic nominal stress, and two material parameters. This equation was evaluated as a Two-Parameter Fracture Criterion for compact and notch-bend specimens. Although the materials analyzed in this paper failed in a ductile manner, the TPFC was able to relate failure stress to crack size and configuration. The TPFC reduces to LEFM for brittle materials. Therefore, the TPFC should be useful to designers who must calculate failure stresses in flawed components.

APPENDIX A

Elastic Stress-Intensity Factors for Notch-Bend and Compact Specimens

The stress-intensity factors for notch-bend and compact specimens have been obtained by previous investigators. In this paper the stress-intensity factors were written in terms of nominal stress, crack length and specimen width (see eq. (2)). This section gives the equations used to express stress-intensity factors in terms of nominal stress.

Notch-Bend Specimens

The stress-intensity factors for three-point bend specimens were obtained from [7] and the function f(a/W) to be used in eq. (6) for L/W = 4 and 8 was

$$f\left(\frac{a}{W}\right) = A_0 + A_1\left(\frac{a}{W}\right) + A_2\left(\frac{a}{W}\right)^2 + A_3\left(\frac{a}{W}\right)^3 + A_4\left(\frac{a}{W}\right)^4 \qquad \text{(A1)}$$

L/W	A_0	A_1	A_2	A_3	A_4
4	1.93	-3.07	14.53	-25.11	25.80
8	1.96	-2.75	13.66	-23.98	25.22

Compact Specimen

The stress-intensity factors for the compact specimen were obtained from [13] and [14]. However, these stress-intensity factors were obtained by boundary collocation analyses on configurations which did not include the

pin-loaded holes. Although the results in reference 14 can be applied over a wider range of a/W than the results from [13], reference 15 has analyzed the compact specimen using a boundary collocation analysis on a configuration which did include the pin-loaded holes. Therefore, the stress-intensity factors from [15] were used in the fracture analysis. The function $f\left(\frac{a}{W}\right)$ to be used in eq.(6) was

$$f\left(\frac{a}{W}\right) = 4.55 - 40.32\left(\frac{a}{W}\right) + 414.7\left(\frac{a}{W}\right)^2 - 1698\left(\frac{a}{W}\right)^3 + 3781\left(\frac{a}{W}\right)^4 - 4287\left(\frac{a}{W}\right)^5 + 2017\left(\frac{a}{W}\right)^6 \qquad \text{(A2)}$$

for $0.2 \leqslant \frac{a}{W} \leqslant 0.8$.

REFERENCES

[1] H. F. Hardrath and L. Ohman, A Study of Elastic and Plastic Stress Concentration Factors Due to Notches and Fillets in Flat Plates, NACA Rep. 1117, 1953. (Supersedes NACA TN 2566.)

[2] H. Neuber, Theory of Stress Concentration for Shear-Strained Prismatical Bodies with Arbitrary Non-Linear Stress-Strain Law, Trans. ASME, Ser. E, J. Appl. Mechs. 28, 544-550, 1961.

[3] J. W. Hutchinson, Singular Behavior at the End of a Tensile Crack in a Hardening Material, J. Mech. Phys. Solids, 16, 13-31, 1968.

[4] J. R. Rice and G. F. Rosengren, Plane Strain Deformation Near a Crack Tip in a Power-Law Hardening Material, J. Mech. Phys. Solids, 16, 1-12, 1968.

[5] P. Kuhn and I. E. Figge, Unified Notch-Strength Analysis for Wrought Aluminum Alloys, NASA TN D-1259, 1962.

[6] J. C. Newman, Jr., Fracture Analysis of Surface- and Through-Cracked Sheets and Plates, Engineering Fracture Mechanics Journal, Vol. 5, 1973.

[7] "Plane Strain Crack Toughness Testing of High Strength Metallic Materials," ASTM STP 410, 1966.

[8] "Fracture Toughness Testing," ASTM STP 381, 1964.

[9] P. Kuhn, Residual Tensile Strength in the Presence of Through Cracks or Surface Cracks, NASA TN D-5432, 1970.

[10] J. G. Kaufman and F. G. Nelson, More on Specimen Size Effects in 2219-T851 Aluminum Alloy, Seventh National Symposium on Fracture Mechanics, 1973.

[11] J. H. Crews, Jr., Elastoplastic Stress-Strain Behavior at Notch Roots in Sheet Specimens Under Constant-Amplitude Loading, NASA TN D-5253, 1969.

[12] A. S. Tetelman and A. J. McEvily, Jr., "Fracture of Structural Materials," (John Wiley and Sons, N.Y.), 1967, pg. 287.

[13] "Review of Developments in Plane Strain Fracture Toughness Testing," ASTM STP 463, 1969.

[14] J. E. Srawley and B. Gross, Stress Intensity Factors for Bend and Compact Specimens, Engineering Fracture Mechanics Journal, Vol. 4, No. 3, Sept. 1972.

[15] J. C. Newman, Jr., Stress Analysis of the Compact Specimen Including the Effects of Pin Loading, Seventh National Symposium on Fracture Mechanics, 1973.

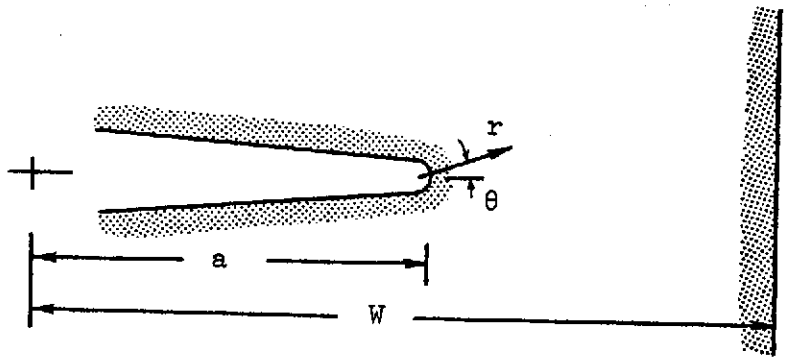

Fig. 1 - Coordinate system for a crack in a finite plate.

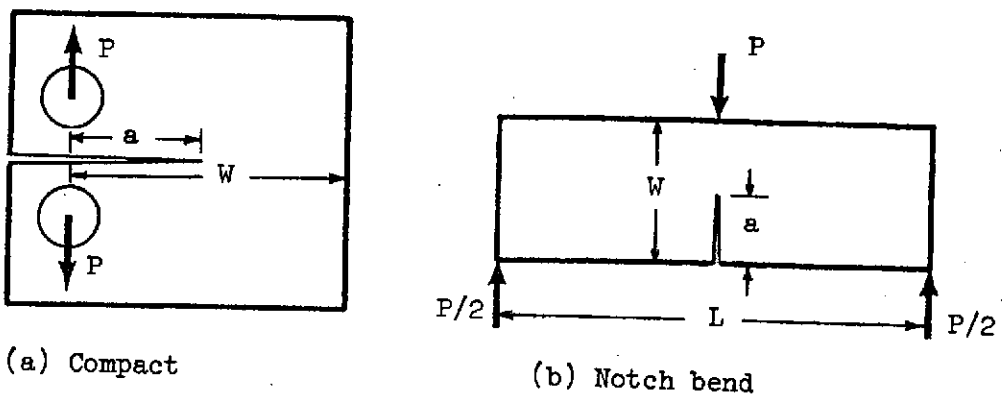

Fig. 2 - Compact and three-point notch-bend specimens.

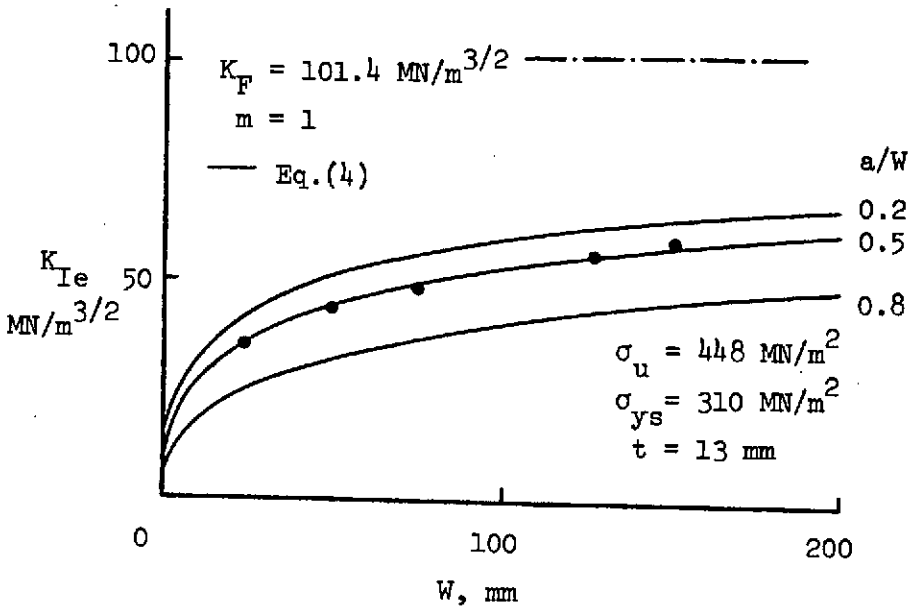

Fig. 3 - Critical stress-intensity factors for 2219-T851 aluminum alloy compact specimens as a function of width.

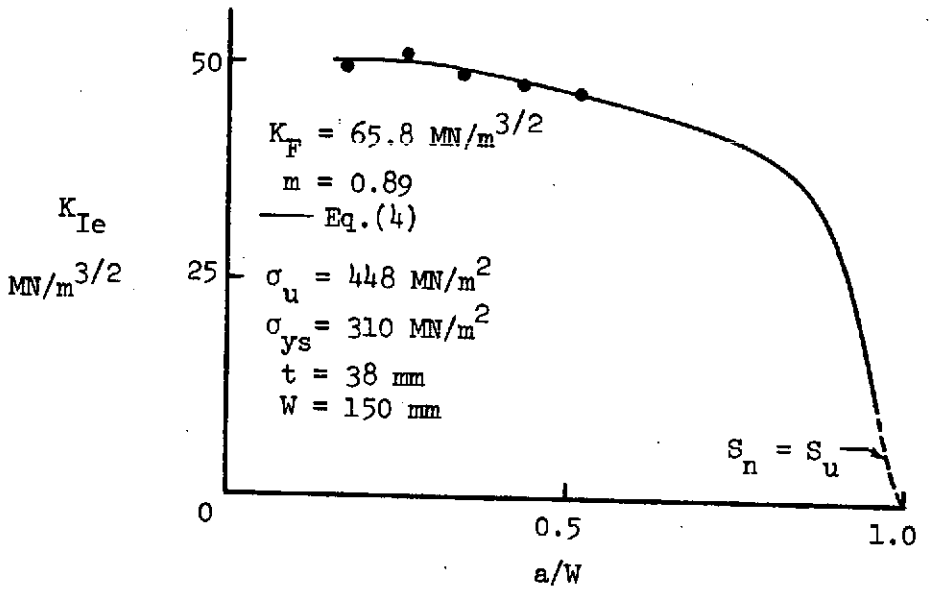

Fig. 4 - Comparison of experimental and predicted critical stress-intensity factors for 2219-T851 aluminum alloy compact specimens as a function of a/W.

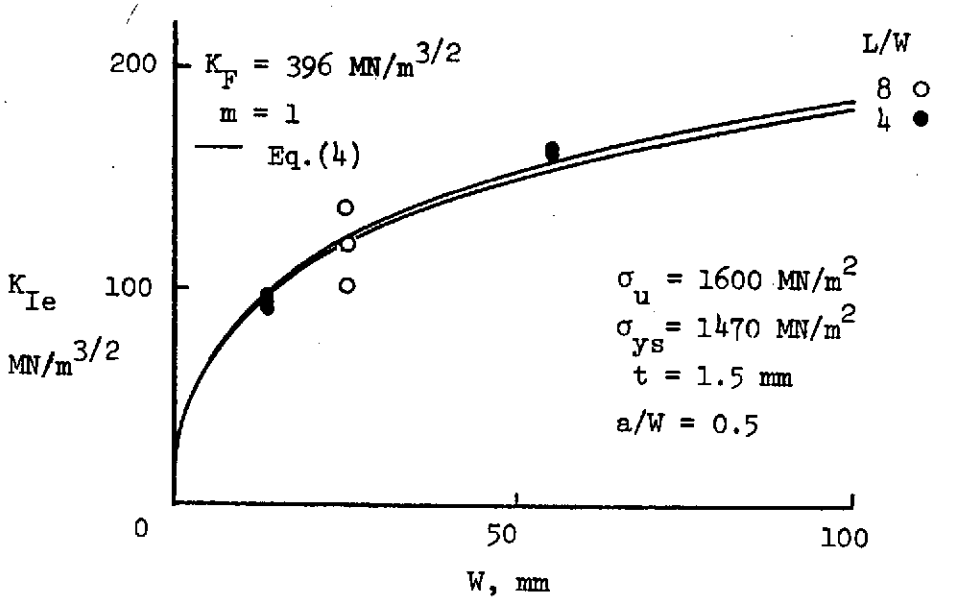

Fig. 5 - Critical stress-intensity factors for 4340 steel three-point notch-bend specimens as a function of width.

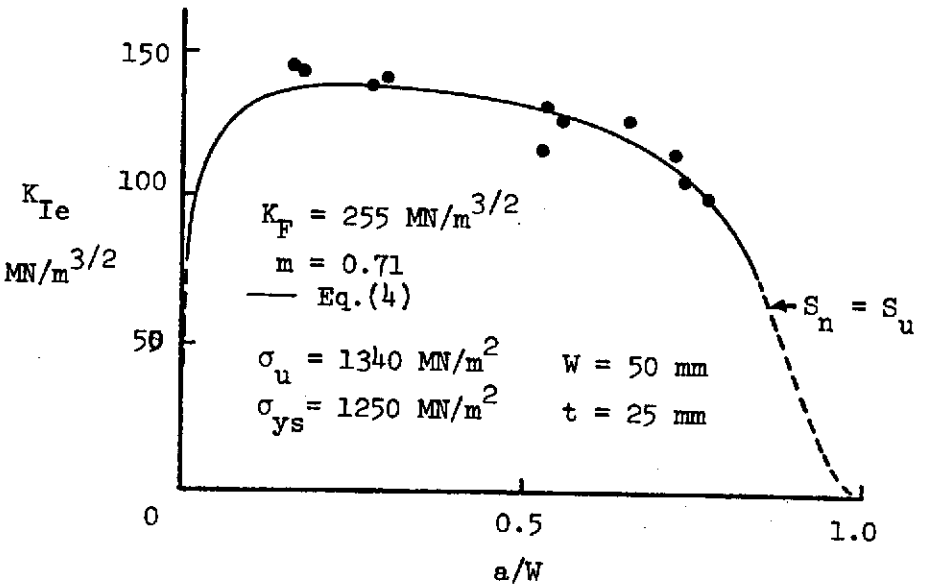

Fig. 6 - Critical stress-intensity factors for 4340 steel three-point notch-bend specimens as a function of a/W.